Chapter 8
Tribolon: Water-Based Self-Assembly Robots

Shuhei Miyashita, Max Lungarella, and Rolf Pfeifer

Self-assembly is a process through which an organized structure spontaneously forms from simple parts. This process is ubiquitous in nature, and its amazing power is documented by many fascinating instances operating at various spatial scales. Despite its crucial importance, little is known about the mechanisms underlying self-assembly and not much effort has been devoted to abstract higher level design principles. Taking inspiration from biological examples of self-assembly, we designed and built a series of modular robotic systems consisting of centimeter size autonomous plastic tiles capable of aggregation on the surface of water. According to the characteristics of the modules composing them, the systems were classified as "passive," "active," and "connectable." We conducted experiments specifically aimed demonstrating the power of behavioral representation of each system with respect to the level of autonomy of its components. We focused mainly on the effect of the morphology (here shape) of the modules, in particular on the yield of the self-assembly process.

8.1 Introduction

Since the breakthrough discovery of DNA by James Watson and Francis Crick more than 50 years ago, there have been enormous advances in our understanding of the material bases of life. Despite the progress, the emergence of life from the local interactions of components (such as molecules, proteins, and cells) remains one of the big mysteries of modern science. Most discussions about life still gravitate around in-depth descriptions and modeling of the interactions between molecules and cells (e.g., through steady-state representations such as reaction pathways). The actual dynamical processes underlying these interactions, however, remain mostly unknown.

The main assumption of this chapter is that by taking a closer look at the region separating life from nonlife, it may be possible to get a better understanding of how

A. Adamatzky and M. Komosinski (eds.), *Artificial Life Models in Hardware*,

the interactions between nonliving entities (such as atoms and molecules) can give rise to life. For instance, the formation of the complex symmetrical protein shells of spherical viruses is a well-studied example of self-assembly. The shell of the T4 bacteriophage (so-called because it infects bacteria) is composed of hundreds of parts and it is not plausible to assume that the instructions for its construction are only contained in the virus' genetic material. This virus consists of about 70 different kinds of proteins and exploits the metabolism of the host cell (e.g., *E. Coli*) to generate around 100 of itself in approximately 40 min. Even more surprising is the fact that if the right kinds of proteins are mixed, the virus can be synthesized in vitro [1, 2], which is truly remarkable for such a complex system.

Although the discussion of whether viruses are living things or not has been controversial ever since, typically, viruses are considered to be nonliving entities, because they cannot reproduce without the help of another organism. As the research documented above shows, the rules that guide the interaction at a local level are simple; the interactions of a large number of entities can lead to the emergence of complex structures, through a process of self-assembly.

8.2 Self-Assembly Robots

Manufacturing technologies and industries heavily rely on robots. For macroscopic objects, industrial robots are not only economical but are also reliable, fast, and accurate. They are widely used in production processes (i.e., pick-and-place car manufacturing robots) and other situations where their environment as well as their task are well defined and no unexpected situations occur. However, as the assembled objects become more complex, conventional engineering technologies hit on a complexity barrier, which entails lower yields and higher fabrication costs.

Recent advances in robotics have, therefore, pointed out the importance of self-assembly for building complex objects, aiming at exploiting the obvious advantages of living organisms, such as their capability to self-configure or self-heal. Modular robots – autonomous machines consisting of typically homogeneous building blocks – promise a viable solution because they have the ability to be highly versatile. For instance, at least ideally, they can reconfigure and adapt their shape according to a given task-environment. Many attempts have been made to realize self-assembling and self-reconfigurable systems. Work has been mainly focused on the design and construction of basic building blocks of a typically small repertoire, with docking interfaces that allow transfer of mechanical forces and moments, and electrical power, and that can also be used for data communication.

The essential issues of how to develop cellular (modular) robotic systems were already described 20 years ago by Fukuda and his collaborators [3, 4]. This work was followed by a more detailed analysis of the kinematics and the metamorphic design of a modular robot inspired by amoebae [5]. Several different types of modular robotic systems, which could morph into desired target configurations (e.g., a snake or a quadruped), were designed by Murata et al. [6–8]. Locomotion of a

reconfigurable modular robot was investigated by Yim [9]. Kotay et al. developed a robotic module which could aggregate as active three-dimensional structures that could move and change shape [10]. Another self-reconfigurable robot was proposed by Rus et al. [11]. This robot could form aggregates by expanding and contracting its shape. A self-contained modular system (it included its own processor, power supply, communication system, sensors, and actuators) was designed by Castano et al. [12]. These modules were designed to work in groups as part of a large configuration. A similar approach can be seen in the work presented by Jorgensen et al. [13], which consists of several fully self-contained robot modules. An autonomous modular robot capable of physical self-reproduction using a set of cubes was created by Zykov et al. [14].

All the robots described above can rearrange the connectivity of their structural units to create new topologies to accomplish diverse tasks. Because the units move or are directly manipulated into their target locations through deliberate active motion, the modular system is called "deterministically self-reconfigurable." The implication is that the exact location of the unit is known all the time, or needs to be calculated at run time.

By contrast, self-assembly systems are "stochastically self-reconfigurable" implying that (1) there are uncertainties in the knowledge of the modules' location (the exact location is known only when the unit docks to the main structure) and (2) the modules have only limited (or no) computational (deliberative) abilities. Pioneering experiments on artificial self-replication were conducted by Lionel and Roger Penrose almost 50 years ago [15]. They presented a mechanical model of natural self-replication in a stochastic environment. Followed by Hosokawa's work [16,17], speculations about the clustering pattern of passive elements were conducted. The Whitesides group revealed different types of self-assembly at small scales [18–21]. Notable ideas about conformational switch were proposed by Saitou [22].

To date, a few self-reconfigurable modular robots relying on stochastic self-assembly have been built (White et al. [23, 24]; Shimizu et al. [25]; Bishop et al. [26]; Griffith et al. [27]). Although in all these systems the units interact asynchronously and concurrently, a certain amount of state-based control is still required for the modules to move, communicate, and dock. Such docking/undocking is one of the main challenges towards the realization of self-assembly systems. Except from molecular self-assembly (see following paragraph), to our knowledge there have not yet been any attempts at exploring stochastic macroscopic self-assembly systems where the parts have only limited (or no) computational (i.e., deliberative) abilities.

It is plausible to assume that self-assembly can also lead to innovation in applications such as macroscale multirobot coordination and manufacturing technologies for microscale devices. By taking tools and methods from nature, many inroads have already been made to utilize self-assembly for the fabrication of structures at molecular scales [28–32]. While they are designing DNA for the elements, Yokoyama assigned molecules for the assembly tasks [33].

8.2.1 The "ABC Problem"

For modular systems smaller than a few centimeters, there are three fundamental problems that still await a solution. These problems relate to actuator, battery (or power in general), and connector technology (henceforth, referred to as the "ABC problem"). When designing systems where a high quantity of modules of small size is desired, solutions for these problems are of particular relevance. First, actuation endows the parts with the ability to move and reconfigure. A common solution is to use electrical servo motors. These actuators, however, are typically big and heavy. Other means of actuation have also been proposed, e.g., pneumatic actuators. Although they are lightweight, they require a source of compressed air (e.g., a compressor). The second problem is concerned with providing power to the actuator(s). A typical solution is to use batteries. Batteries, however, are problematic, because they are only able to provide power for a limited period of time. Furthermore, their initial charge may vary which leads to heterogeneously actuated modules. Another popular solution involves propagating current through the binding locations. Unfortunately, this solution has the drawback that the alignment of the connecting points has to be very precise. In addition, such modules cannot segregate from the main structure, which prohibits this way of powering for mobile type robots. The third problem is the connection mechanism enabling the modular parts to dock to each other. Binding is crucial for reorganization and for a desired structure to hold. The most common ways of binding are magnets and mechanical latches.

There is a strong interdependency between these issues. The requirements of the connection mechanism as well as the actuator are partly determined by the weight of each module. The heavier the modules, the more force needs to be applied to the binding location. In addition, the actuators have to apply larger torques to displace the modules. The use of more powerful components in general leads to even heavier modules. Also, the power consumption increases as a result of stronger connection mechanisms and actuators. Surprisingly, small size and weight reduction of modular parts is not a good way to solve this problem, because not only does the power/weight ratio of the most common actuators decrease with a reduction in size, but also so does the strength/weight ratio of common connectors. This implies that the most common ways of actuating, powering, and connecting modular robots cannot be applied to small-sized entities. It follows that novel solutions to the ABC problem are necessary to make progress in small-scale modular robotics.

8.3 Tribolon: Water-Based Self-Assembly Robots

In this section, we introduce our three water-based self-assembly systems called Tribolon[1]: a "passive" system, an "active" system, and a "connectable" system (in Sects. 8.3.1, 8.3.2, and 8.3.3, respectively). The first two systems float on water, whereas the third one is immersed in water.

[1] The name is derived from Tribology. Movies and pictures are available from `http://shuhei.net/`

8.3.1 Passive Tile Model

The first prototype of our self-assembly robot was developed in 2005. The model consists of flexible plastic tiles (base plate) floating in a water tank (Fig. 8.1). Figure 8.1 a shows one of the proposed floating tiles (0.2 g, $22 \times 22 \times 2$ mm). We constructed three different types of tiles: squares, circles, and squares with rounded corners (rounded squares). A vertically oriented magnet was attached to the bottom of each base plate such that either the North pole or the South pole was directed upwards (depending on the color of the elements). To produce turbulence on the water surface and to provide the system with the energy necessary to drive the self-assembly process, we attached two vibration motors to the sides of the water tank.

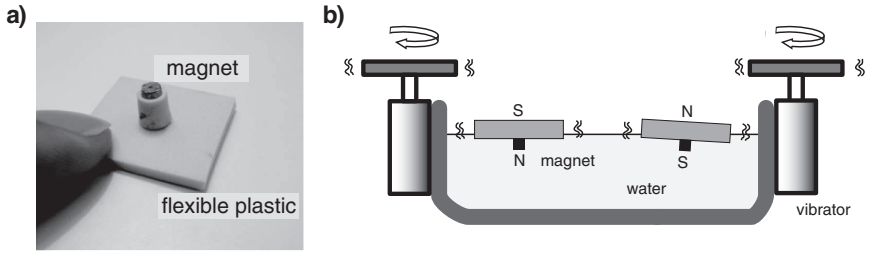

Fig. 8.1 The experimental setup for assembly of passive tiles. (**a**) A vertically oriented magnet was attached to the bottom of each base plate. (**b**) The stirring of water generates random, fluctuating forces providing the system with the necessary energy for assembly

For the experiments, we built 30 blue tiles (N) and 30 pink tiles (S) for each shape. In what follows, we summarize the results of our experiments as a function of the type of shape used.

- *Square* (Fig. 8.2 a): The tiles change their relative positions by sliding along their edges. The connection between two tiles is strong, that is, a relatively large amount of energy is required to break the connection. The clusters formed are stable and rather static, that is, the modules tend to stay in the same configuration for a prolonged period of time.
- *Circle* (Fig. 8.2 b): The tiles easily change their relative positions by moving along the edges of tile pairs. In most cases, several small groups are formed. The speed of aggregation is high, but the structures created are unstable and easily disintegrate due to turbulence; the results are configurations which wax and wane.
- *Rounded square* (Fig. 8.2 c): This type of tile combines the positive characteristics of the squared and the circular tile; that is, stable connections and flexible change of position. The lattice structure is reached rapidly and is stable for a prolonged period of time.

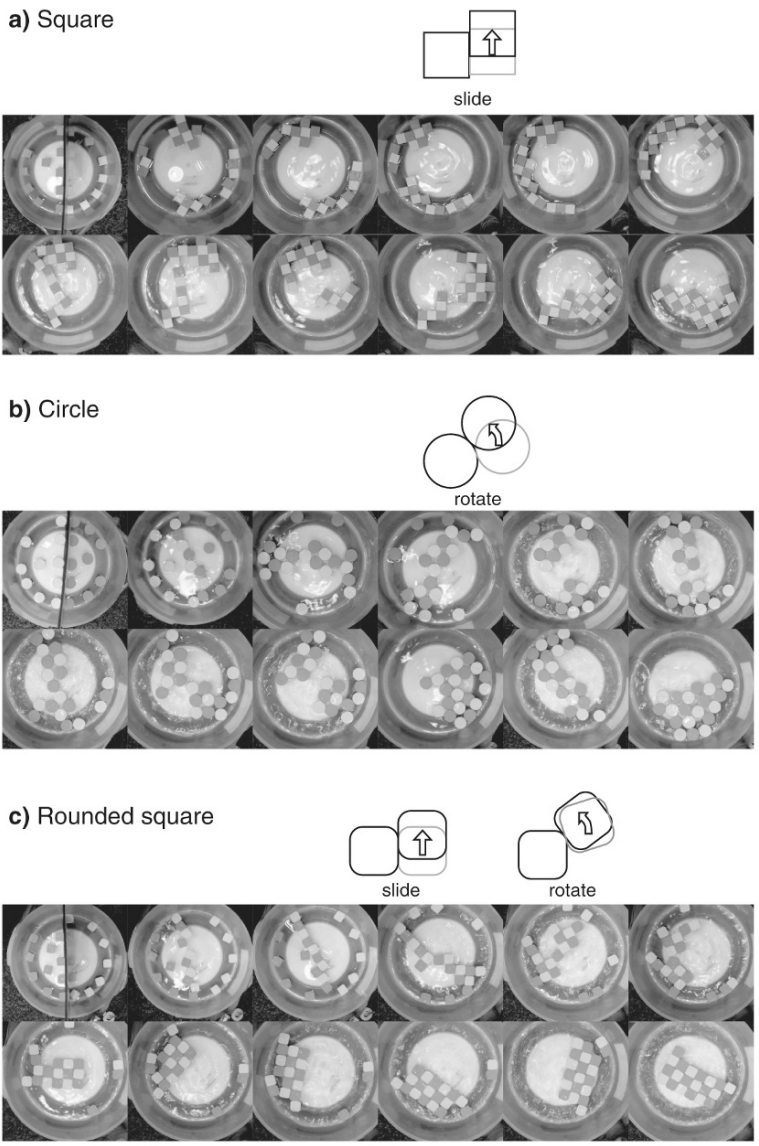

Fig. 8.2 Each shape displays a distinct behavioral pattern. The larger the curvature of the corners of the tiles, the faster the aggregation speed and the less stable the final configuration

As can be inferred from the above summary, each shape displays a distinct behavioral pattern. The larger the curvature of the corners of the tiles, the faster the aggregation speed and the more unstable the final configuration. This study effectively demonstrates how a small change of (local) morphology can induce a change of behavior affecting the global configuration of the system.

8.3.2 Self-propelled Model: Tiles with Vibration Motors

The word self-assembly implies that the involved elements or parts assemble spontaneously without external intervention (i.e., they are autonomous). It follows that the ability to "locomote" (i.e., to move around) is an important prerequisite for self-assembly. To address this requirement, we equipped each module with a vibration motor (pager motor).

8.3.2.1 Experimental Setup

Each module was built with flexible plastic. A small vibration motor was positioned on top of the tiles, and a permanent magnet was attached to the module's bottom surface (Fig. 8.3 a). The magnet was made of Neodymium, which had a surface magnetic flux density of 1.3 T. Because the actuating system had to be small and controllable, we chose vibration motors. This allowed the modules to move around in their environment like Brownian particles. Rather than using batteries for each module, we opted to supply electricity through a pantograph that draws current from a metal ceiling (aluminum) (Fig. 8.3 b) (a similar technique is used by cars in amusement parks, Fig. 8.3 c). This solution has several advantages: (1) all modules receive the same power, which is necessary because all modules should be identical and (2) the modules can be very lightweight. When an electrical potential was applied to the ceiling plate, current flowed through the pantograph to the vibration motor returning to ground via platinum electrodes immersed in the water. Salt, $83.3\,\mathrm{g\,l^{-1}}$ was added to the water to make it conductive (electrolyte). The weight of each module was approximately 2.8 g with a size of about 3 cm. As depicted in Fig. 8.3 b, the modules could tilt, inducing rather large fluctuations in the current flowing through the motors.

8.3.2.2 Experiment 1: The Ability to Express Various Behaviors

Experiments carried out with various types of modules are shown in Fig. 8.4. We used different types of primitive shapes, such as circles or triangles, and demonstrated their ability to express various behaviors in each combination. Three modular systems were powered via the ceiling (c, e, f), while the others were powered through a wire (a, b, d, g). Some of the modular configurations were initialized manually (a, b, d, g). Moreover, not all the modules contained a vibration motor (only the modules with a letter "V").

- *Reel* (Fig. 8.4 a): A vibrating module can reel a string of modules. Circular modules whose magnetic North points upwards and modules whose magnetic North points downwards rotate in opposite directions.
- *Gear* (Fig. 8.4 b): This example shows how far the rotational movement generated by the vibrating modules can be transferred.

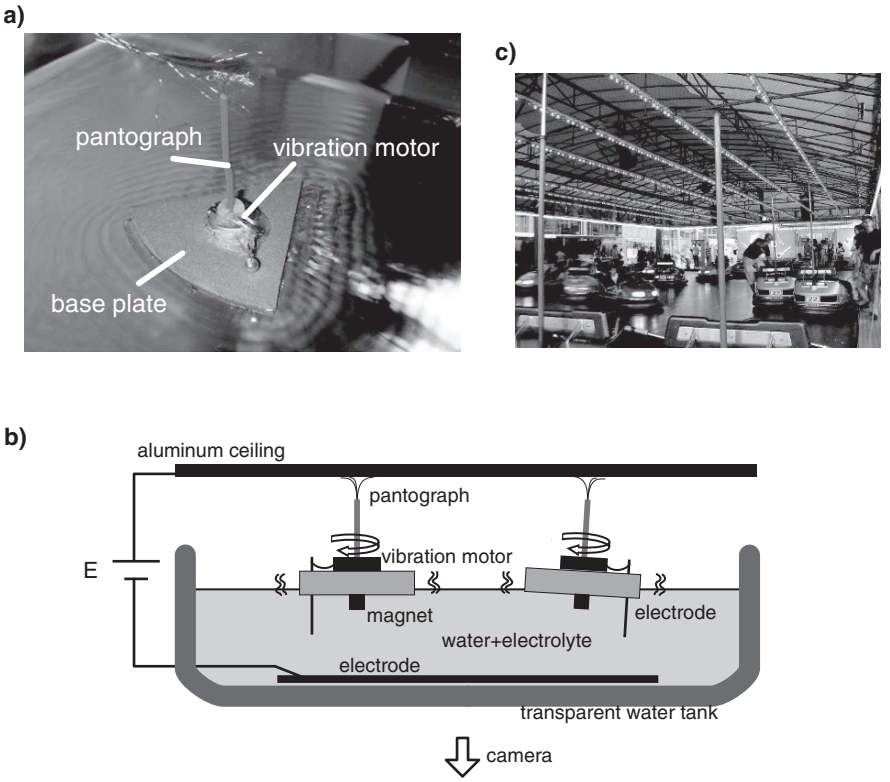

Fig. 8.3 Experimental setup. (**a**) Snapshot of a Tribolon module. (**b**) Illustration of the experimental environment with two modules. (**c**) Bumping cars in an amusement park, which employ a similar technique

- *Bike* (Fig. 8.4 c): A triangular vibrating module follows a wall. The addition of two circular modules close to it, turns them into "wheels" and the whole cluster starts following the wall.
- *Planets* (Fig. 8.4 d): A vibrating module placed manually attracts a small module through a magnetic force. The movement of the big module forces the small module to rotate around itself (rotation and revolution).
- *Dimer* (Fig. 8.4 e): All the three modules contain a vibration motor. Two modules (S) "chase" one module (N). After a while, one module reaches a stable position and the other modules stops the chase.
- *Lattice* (Fig. 8.4 f): All modules contain a vibration motor. Only the circular modules rotate, while the square ones stop moving.
- *Rotation* (Fig. 8.4 g): A triangular module can rotate around a circular module following its edge. The circular modules slide their positions and push the edge of the triangle module and generates a rotational movement.

It has to be mentioned that the reactions responsible for the structuring of the system act at a strictly local level, that is, all behaviors described above emerge

spontaneously and autonomously through a decentralized process. Thus, by contrast to traditional manufacturing processes, less control is required for the assembly. The process and the configurations are also more robust against unforeseen damage, implying that the system is largely capable to recover from failure and external disturbances.

In addition, our simple and cheap experimental setup makes it suitable as an educational tool. It not only helps people grasp difficult concepts such as "open, nonequilibrium dynamical system," but also provides a starting point for thinking about natural systems.

8.3.2.3 Experiment 2: Circular Section Shape Module

A "shape" can be described by indicating angles and the length of the edges forming them. One of the inevitable problems when we discuss about shapes is that a change of one parameter can lead to changes in another parameter, which makes it hard to discuss the implications of a single parameter change. To study this issue, we designed a set of pie-shaped modules (wedges) spanning an angle of α degrees. A permanent magnet was attached, oriented orthogonally to the module's main axis (Fig. 8.5 a). Snapshots taken from three experiments using such six modules (for $\alpha = 60^\circ$) are visualized in Fig. 8.6.

In each experiment, a different (constant) electric potential was applied between the ceiling plate and the bottom submerged electrode causing the Tribolon modules to aggregate in various ways. In the experiment reproduced in Fig. 8.6a, we applied a potential of $E = 7$ V. The modules first moved along random paths vaguely reminiscent of Brownian motion. After some time ($\approx$9 s), through magnetic attraction, some of the modules were pulled to each other forming two-unit clusters (denoted by X_2; X_i stands for the state of a cluster consisting of i modules). These clusters further combined to generate a four-unit cluster (X_4), then a five-unit cluster (X_5), and eventually a six-unit cluster (X_6) (sequential self-assembly; Fig. 8.6). Once this final state was reached, the whole circular structure started to rotate counter-clockwise at an almost constant speed, forming a propeller-like structure. A plausible explanation for this "higher level functionality" can be found in the intermittency of the contact of the pantograph with the aluminum ceiling (due to the stable configuration of the six-unit cluster on the water surface; see Fig. 8.6 b), which in turn lead to a pulsed current flow.

In the snapshots reproduced in Fig. 8.6 b, the potential was set to $E = 8$ V. As a result of the higher potential, the motors vibrated at a higher frequency, increasing the likelihood of segregation of clusters while decreasing the likelihood of aggregation. Most of the time, all types of clusters disintegrated shortly after formation, exception made for the six-unit cluster (X_6) which, due to its symmetry, proved to be a stable structure. It is important to note that the formation of the six-unit cluster at $T = 98$ s was accidental (one-shot self-assembly). This tendency, suppressing intermediate states, is thought to be a potential solution to the yield problem (see Sect. 8.3.2.4).

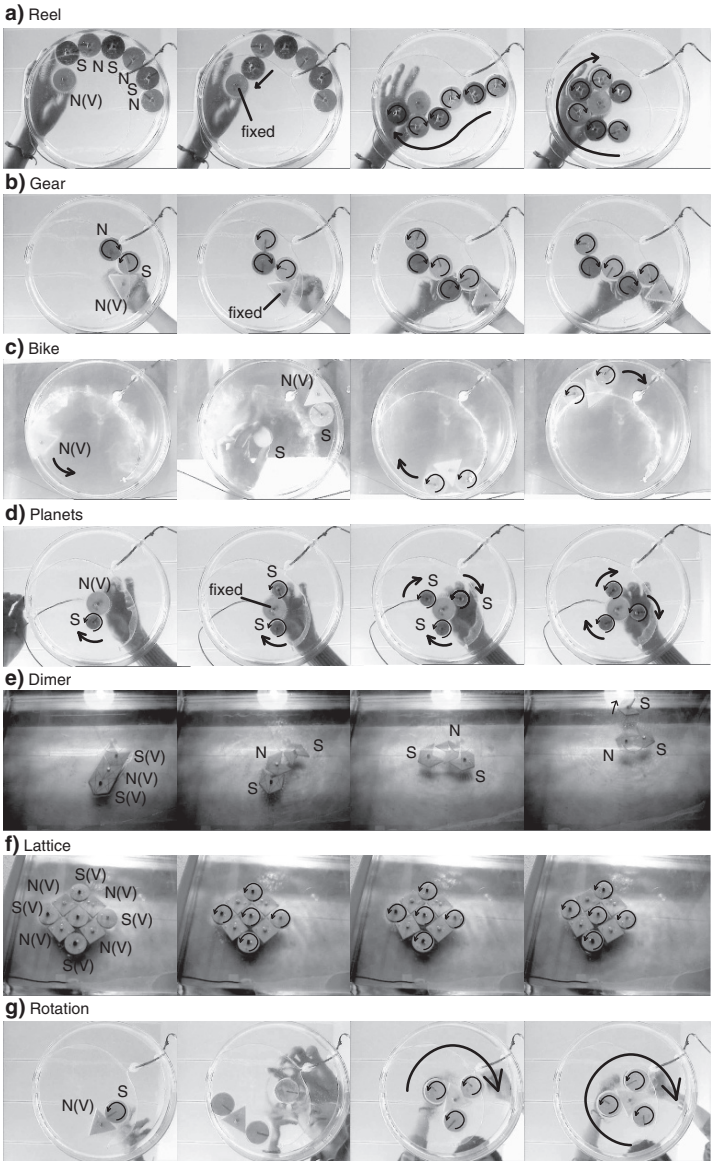

Fig. 8.4 The ability to express various behaviors. Three modular systems were powered via the ceiling (**c, e, f**), while the others were powered through a wire (**a, b, d, g**). Some of the modular configurations were initialized manually (**a, b, d, g**); not all the modules contained a vibration motor (only the modules with a letter "*V*")

The snapshots in Fig. 8.6 c were obtained by applying a potential of $E = 9$ V. This potential induced the vibration motors to vibrate even faster making the formation of a six-unit cluster unlikely. In fact, even for prolonged experiments no clusters

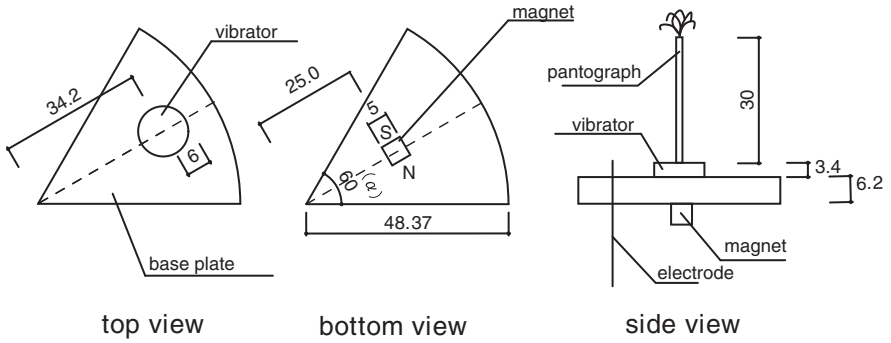

Fig. 8.5 Schematic representation of a Tribolon module (units: (mm), (degrees)). Each module weighs approximately 2.8 g and covers an area of 12.25 cm^2. The angle spanned by the circular sector is $\alpha = 60^\circ$

could be observed (random movements). We confirmed this result by initializing the experiment with modules arranged in a circular configuration consisting of six units (the desired configuration); as expected, the cluster was unstable and disaggregated shortly after the start of the experiment.

8.3.2.4 Yield Problem

The problem of producing a desired configuration in large quantities (while avoiding incorrect assemblies) is known as the "yield problem" and has been studied in the context of biological and nonbiological self-assembly systems [16,17]. For example, let us assume that the self-assembly process is initialized with 12 modules – each one a pie-shaped wedge spanning 60° – with the objective to form two complete circles consisting of six modules each. In fact, the likelihood that the system actually settles into the desired configuration (a circle) is rather low (Fig. 8.7). In this respect, suppressing the probability of remaining in intermediate states may help reducing the occurrence of this problem, in our case Fig. 8.6 b.

An essentially analogous problem is investigated in the context of DNA folding, where one of the objectives is to increase the yield rates of the self-assembly process [29]. Similarly, a lot of research effort is being devoted to the development of high-yield procedures for integration and mass manufacturing of heterogeneous systems via self-assembly of mesoscopic and macroscopic components [34–36].

8.3.2.5 Mathematical Analysis

We studied the behavior of our self-assembly system using kinetic rate equations derived from analogies with chemical kinetics [16]. For the analysis, the quantity of every intermediate product is represented by a state variable.

a) Sequential self-assembly (E=7V).
The first modules form two-units clusters (X2) which eventually assemble into a six-units cluster (X6).
Once this final state was reached, the whole circular structure rotates counter-clockwise at constant speed.

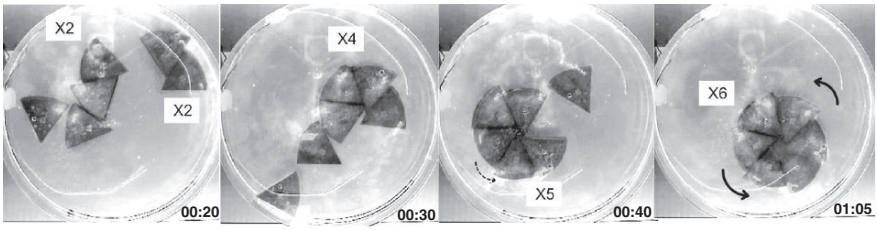

b) One-shot self-assembly (E=8V).
Most clusters are unstable. The six-units cluster (X6), however, is a stable symmetric structure.

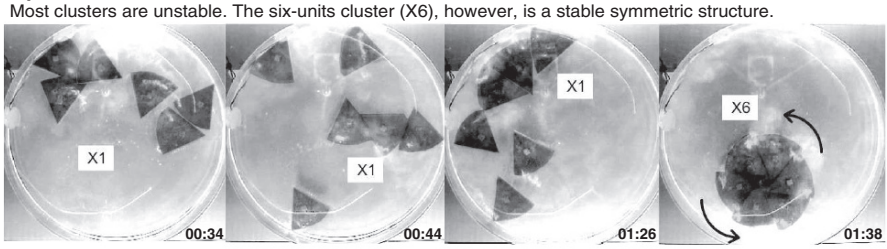

c) Random movements (E=9V).
All kinds of clusters are unstable and quickly disaggregate.

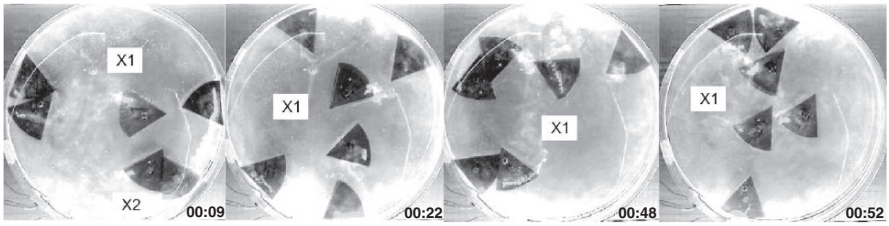

Fig. 8.6 Experimental results. Self-assembly process as a function of the applied electric potential E

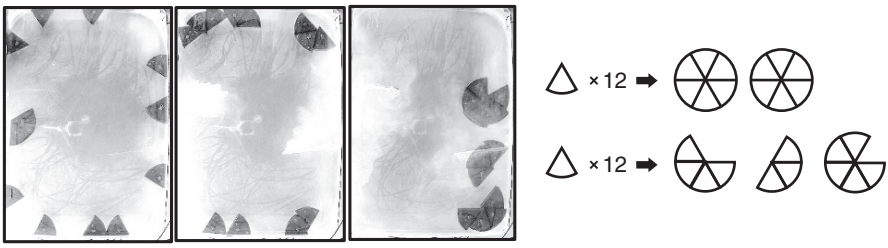

Fig. 8.7 Yield problem and stable clusters. Twelve circular sectors X_1 can aggregate into two X_6 clusters. In most cases, however, the modules organize themselves in more than three clusters. The yield in the upper part of the figure is 100%, the one in the lower part is 0%

Figure 8.8 displays the change over time of the number of clusters obtained by solving the system of difference equations with initial condition $X_1 = 100, X_i = 0 (i \in \{2...6\})$ (more detail, see [37]). As can be seen, $X_5(t) > X_6(t)$, which exemplifies the yield problem. The yield rate of each cluster is listed on the top-right of the figure as a circle graph.

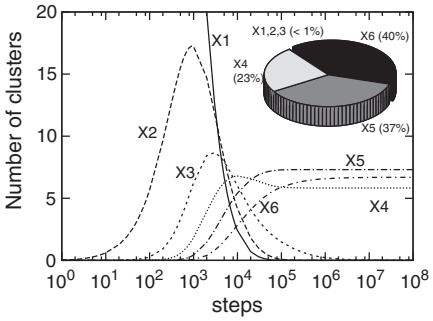

Fig. 8.8 Number of clusters as a function of time. The yield problem is evident from the fact that at steady-state $X_5(t) > X_6(t)$

Figure 8.9a, b shows how shape changes affect the yield of the self-assembly process. The yield rates are normalized by multiplying them by the number of units required to construct a full circle (i.e., in the case of $\alpha = 60^\circ$, the factor is 6; in the case of $\alpha = 180^\circ$, the factor is 2), and plotted as a function of the angle α. As seen in the figure, the yield rate falls off linearly with the angle. This result can be explained by considering that the number of clusters required to form the desired structure is inversely proportional to the angle. An additional point is that clusters formed by an even number of units show better yield rates. In Fig. 8.9b, we plotted the yield rates on a logarithmic scale. As expected, the narrower the angle, the worse is the performance of the system. Interestingly, the relationship between yield rate

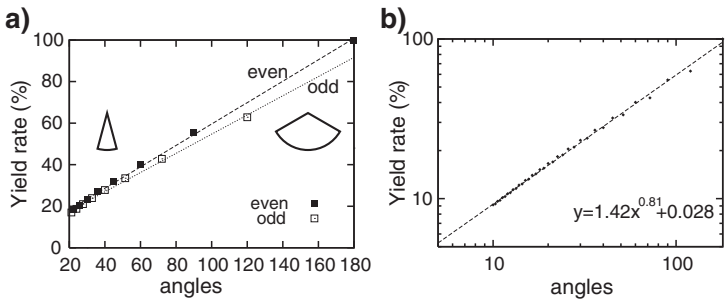

Fig. 8.9 Yield rates as a function of the angle spanned by the pie-shaped wedge; (**a**) linear scale and (**b**) logarithmic scale. Interestingly, the relationship between yield rate and angle follows a power-law with a scaling exponent of 0.81

and angle follows a power-law with a scaling exponent of 0.81. Although this will require additional investigation, we hypothesize that this relationship is the result of the shape of the module (in this case the circular sector with an orthogonally attached magnet).

8.3.2.6 Homogeneous *vs* Heterogeneous

Biological systems consist of many different types of components. We speculate that in any minimal setting, there must exist a suitable level of heterogeneity. In our circular cut model, we considered the angle α to be an adequate parameter for the heterogeneity of the system, i.e. the 60° module and 120° module should be treated as different (heterogeneous) modules. However, once two 60° modules connect, a 120° module forms, which is obviously equivalent to a 120° module. The lesson learnt from this example is that the concepts "homogeneous" and "heterogeneous" cannot be separated from the context in which they are used.

8.3.2.7 Passive or Active?

An additional issue addressed by our model is the distinction between "passive" and "active." For instance, it may be possible to achieve the same behaviors by applying an external rotational magnetic field instead of attaching a vibration motor to each tile. Strictly speaking, active tiles should, therefore, be treated like passive tiles implying that the distinction tends to be trapped by frame of reference problem [38]. The essential difference between the active and the passive system is the type of asymmetries that the two systems can produce.

8.3.2.8 Hierarchical Levels of Functionality

Let us return to the question formulated in the introduction: can we build nonbiological (modular) systems that self-assemble like biological ones? By carefully mapping the interaction networks of the approximately 70 proteins involved in the assembly of the T4 phage, one can observe that the aggregation processes are extremely well organized [1]. For instance, a protein A can only dock on a protein *B* by first coupling with a protein C: $\mathrm{A} + \mathrm{B} + \mathrm{C} \rightarrow \mathrm{AC} + \mathrm{B} \rightarrow \mathrm{ABC}$. It follows that through coupling with protein C, protein A can acquire a different level of functionality, which then enables the interaction with protein B. We assume that this kind of interaction networks can lead to the emergence of multiple levels of functionality, which play a crucial role in many morphogenetic processes. The formation of a propeller-like rotating aggregate (Fig. 8.6 a, b), a bike pattern (Fig. 8.4 c), or a rotation configuration (Fig. 8.4 g) are instances of what one might call "emergent functionality."

8.3.2.9 The Meaning of Morphology

Although the shapes tend to attract attention, an essential role is also played by the distribution of the body from the "origin of the force" (here: magnets). For instance, by shifting the position of the magnets closer to the rounded edge and after perturbing the water, the modules tend to form dimers (two-clusters), orienting the rounded edges towards each other instead of forming a circle (Fig. 8.10 a). This is due to the fact that the configuration is potential, energetically more stable than a full circle (neglecting the dynamic part of the energy). This example seems to indicate that it may not be adequate to perceive this change as a shift of the magnet, but as changing the entire morphology (from the "force source," Fig. 8.10 b). It follows that the reason of the difficulty in achieving lightweight actuators is equivalent to changing the entire morphology.

8.3.3 Connectable Model: with Peltier Connector

To make a step towards highly autonomous lightweight systems, we propose a model incorporating a novel connection mechanism: the water close to the docking interface of one module is frozen to ice, building a local bridge to another module.

8.3.3.1 Peltier Freeze–Thaw Connector

The core of our connector is the Peltier heat pump – a double-faced cooling–heating device that can transfer thermal energy from one side of the device to the other, with consumption of electrical energy. We used the Peltier device to freeze (and thaw) the water between two modules and thus, realize binding (and unbinding) between modules. The polarity of the current applied to the device defines which side is cooled down or heated up. The device consists of different types of semiconducting materials that are connected in series to take advantage of the so-called thermoelectric or Peltier effect. This effect is the direct conversion of an electric voltage into a temperature difference and vice versa, and allows the element to work as a heat pump. Peltier devices are available in various sizes. For our purpose, we used an 8×8 mm element that weighs 0.8 g. Theoretically, the Peltier heat pump can induce a temperature difference of up to 72°C while consuming approximatively 2.60 W. One particular advantage of this type of intermodule connection mechanism is that the absence of mechanical parts makes it scalable. The fact that the connector is devoid of moving parts makes it also intrinsically less prone to failures. One disadvantage is that in order to sustain the connections, energy has to be supplied permanently to the heat pump. For the detachment process, however, there is no need to supply energy because the ice melts when it is not cooled down; moreover, the heat flow from the hot surface supports the thawing process speeding it up.

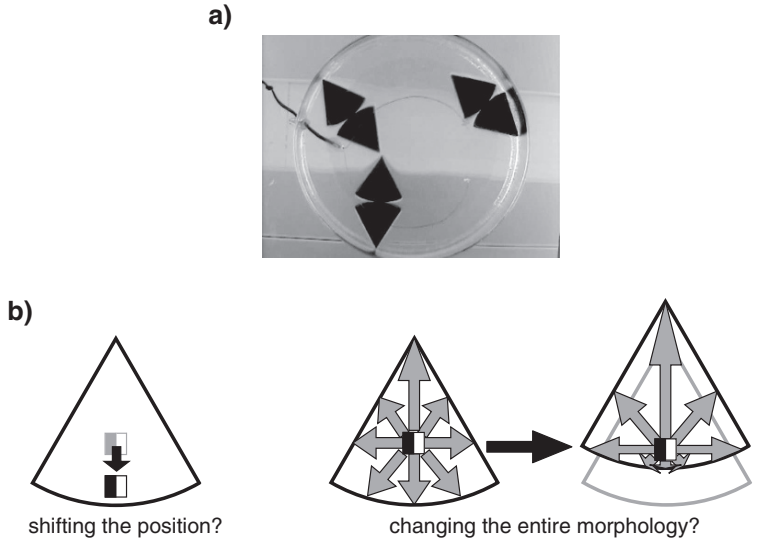

Fig. 8.10 Meaning of morphology. (**a**) Clusters generated by modules with magnets, whose positions were shifted to the rounded edge. (**b**) Shifting the position of a magnet sometimes leads to the result equivalent to the changing the entire morphology

8.3.3.2 Experiment 1: Kite-Shaped Model

The experimental setup was composed of a power supply, a metallic ceiling, a water tank, and six modules immersed partially in water (Fig. 8.11). Each module consisted of a kite-shaped wedge made of flexible plastic (acrylnitrile butadene styrene; ABS) spanning angles of 60° and 30°. The modules (H: 13 mm, L: 30 mm) contained a permanent magnet oriented orthogonally to their main axis to attract or repel other modules (Fig. 8.11 a). A vibration motor was used to endow the modules with a minimal locomotive ability which allowed the modules to move randomly around – vaguely reminiscent of Brownian motion. Rather than using batteries, electricity was supplied to the modules through a pantograph that drew current from a metal ceiling. This solution not only led to lightweight modules ($m = 6.0$ g), but it ensured that all modules received approximately the same amount of energy in a particular experiment.

When an electrical potential was applied to the metallic ceiling plate, current flowed through the pantograph to the vibration motor returning to ground via the platinum electrodes immersed in the water (8 % concentration of electrolyte (salt) was added to the water to make it conductive). To speed up the connection between two modules, the water in which the modules moved was cooled down to approximately -3°C (due to the concentration of salt this was slightly higher than the freezing temperature). Two diodes were used to switch the direction of the current. Current flowed either through the Peltier element or the vibration motor depending on the direction of the voltage applied to the system (Fig. 8.11 c, switch).

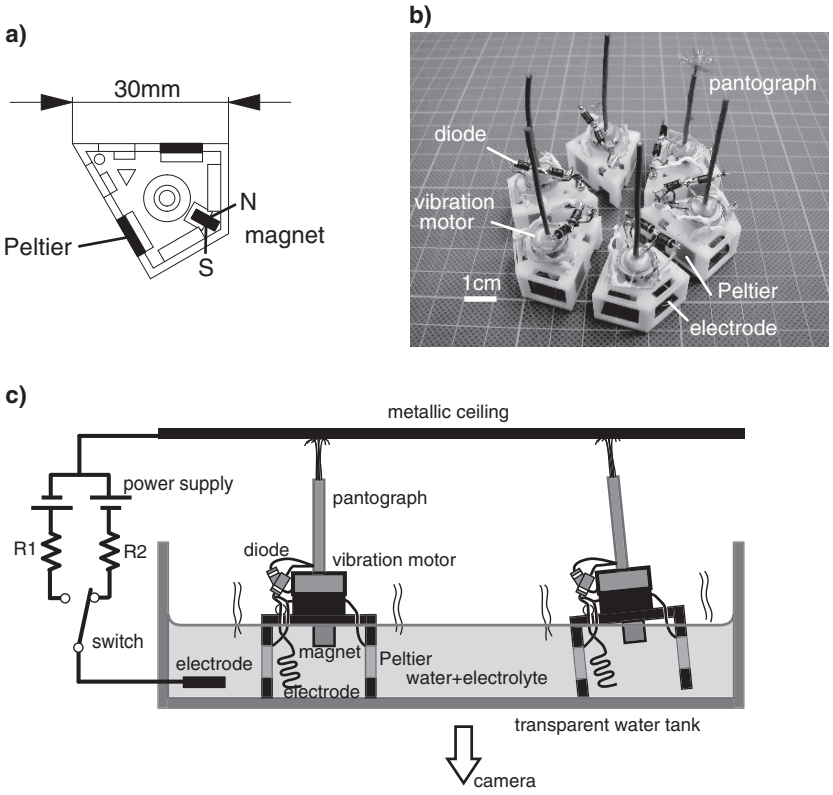

Fig. 8.11 Experimental setup for connectable model. We used the Peltier device to freeze (and thaw) the water between two modules and thus realize binding (and unbinding) between modules. (**a**) Schematic illustration of a module (*bottom view*). (**b**) Picture of six modules. (**c**) Experimental setup with two modules

We first carried out experiments to test the reliability of the connector and to investigate the reconfigurability of our self-assembly system. The result is shown in Fig. 8.12. In the beginning of the experiment, the modules were placed in the arena (Fig. 8.12 a) and arranged by hand to form a hexagonal shape (Fig. 8.12 b). Voltage was applied via the metallic ceiling (Fig. 8.12 c). After 1 min, all six modules were connected to each other forming one unit (Fig. 8.12 d). We then flipped the polarity of the current supplied through the pantograph. The Peltier connectors stopped cooling and the vibration motors started to vibrate causing a disassembly of the hexagonal shape into six separate modules (Fig. 8.12 e). As a result of the vibrations of the motor, the modules moved around in the arena where they eventually got magnetically attracted by another module and started to form triangles (Fig. 8.12 f, g). The experiment was considered completed when the six modules had formed two triangles (Fig. 8.12 h).

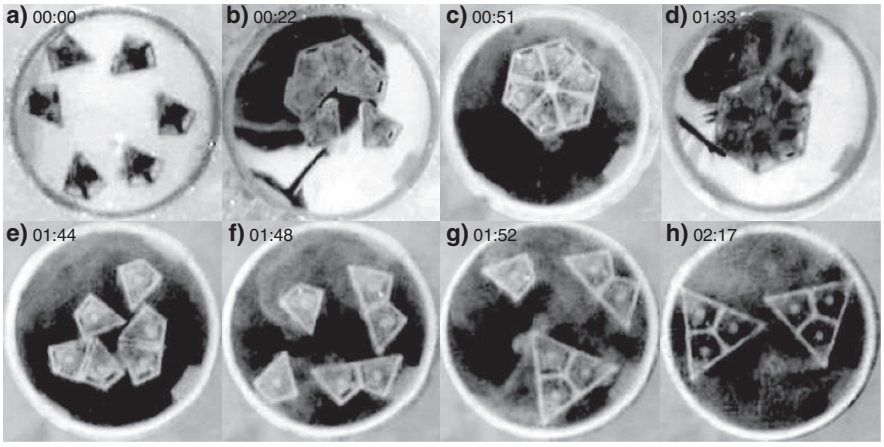

Fig. 8.12 Snapshots of the experiment. A frozen hexagonal module split up into six kite-shaped modules and formed two triangular modules

We conducted the experiment several times. For sufficiently long waiting times T, we always observed two different ways of convergence to the final states: one is in Fig. 8.12 h (two 3-clusters), the other is three 2-clusters (not on the picture, yield problem).

8.3.3.3 Experiment 2: Hinge-Connected Chain Model

The outcome of the experiments described in Sect. 8.3.3.2 led to the question of how to take our modular system to another level of operation. To answer this question, we added permanent magnets to each module. Because with many modules the outcome of this change was not easy to anticipate, we built a new type of module. Each module was physically linked through hinge joints to two modules, forming a chain (Fig. 8.13, $m = 12.8$ g). By taking inspiration from protein folding, we expected a drastic reduction of dimensionality of the search space. The main advantage of this implementation is that it avoids a crucial problem: the increased number of magnets generates undesired configurations. Note that the positions of all the other magnets were replaced and rearranged. Only the center module (colored in red, Fig. 8.13 b) had a large magnet oriented orthogonally to the symmetry axis. The other small cylindrical magnets were oriented vertically – "S"outh poles attracting "N"orth poles and vice versa. As in the modules described in the previous section, diodes were used to direct the current flow. Depending on the polarity of the applied voltage, current only flowed either through the Peltier elements (12 V) or through the vibration motors (10 V).

Snapshots from a representative experiment are shown in Fig. 8.14. At the beginning of the experiment, we arranged by hand two chains of three modules each to form a hexagonal shape (Fig. 8.14 b). Voltage was applied to the system so that

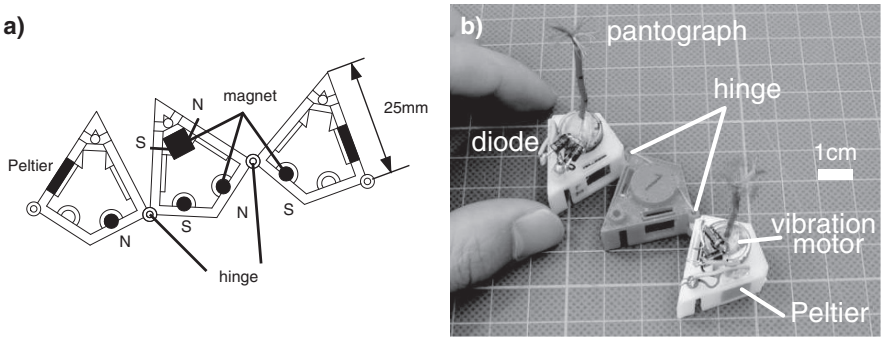

Fig. 8.13 Chain model. (**a**) Schematic illustration of a chain. (**b**) Picture of a chain. Three modules are connected by hinges

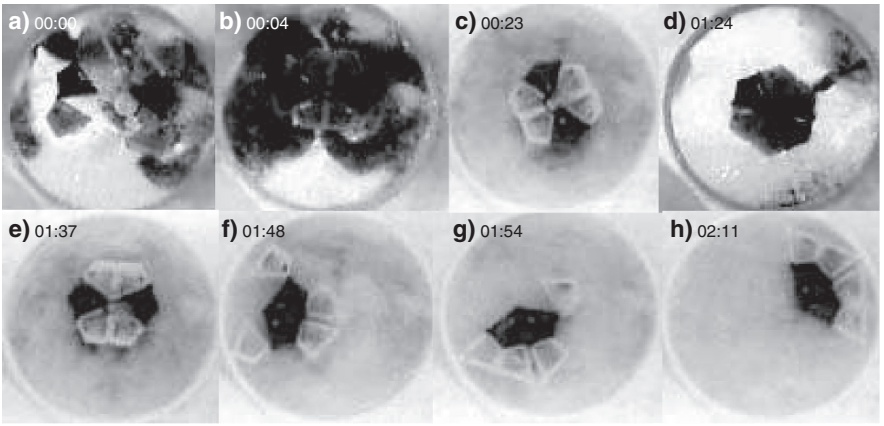

Fig. 8.14 Snapshots of the experiment with chain modules. A frozen hexagonal module split up into two chain modules and two magnetically connected triangle chains were obtained

the Peltier elements were powered (Fig. 8.14 c). After 1 min, an ice layer built up between the modules causing them to attach to each other yielding one single piece (Fig. 8.14 d). We then inverted the polarity of the applied voltage and let the current flow to the vibration motors (Fig. 8.14 e). The ice melted and the modules altered their configuration guided by the magnetic forces (Fig. 8.14 f, g). The transformation was completed in a minute, and two magnetically connected triangle chains were obtained (Fig. 8.14 h).

The success rate of the reconfiguration just described was not as high as expected. We suspect that the low yield rate was mainly due to a design problem: the position of the large magnet was too close to the edge of the module. Therefore, a rather strong movement of the modules was required to induce a disassembly of the initial hexagonal configuration.

The main implication of the two experiments described in this Sect. 8.3.3 is that the restriction of the geometric constraint of modules, in other words, the "dimensionality reduction" of the reconfiguration problems enables the system to transit to a different level of functionality, bringing the modules to magnetically connected triangular clusters, while avoiding undesirable formations (yield problem).

8.3.4 Scale-Free Self-Assembly: Size Matters

The size of 1 cm is a critical size for self-assembly systems. For objects in water at the millimeter scale, viscosity is as important as inertia (the Reynolds number, that is, the ratio of inertial forces and viscous forces, is ≈ 1). It follows that objects smaller than that size are affected more by viscous forces whereas larger objects are affected more by inertial forces. For objects on the order of 1 µm or less, such as bacteria, diffusion is a more effective way of locomotion than active propulsion (e.g., swimming bacteria are slower than diffusing molecules [39]).

In Fig. 8.15 a, 0.5 mm size plastic particles are shown. When mixed with water and shaken, they tend to automatically form three layers which are dominantly affected by (1) static charge on the particles, (2) static charge on the wall, and (3) gravity. As can be seen in Fig. 8.15 b, several number of spherical clusters were generated. We hypothesize that through the mixing and shaking, tiny air bubbles are created in the water. The air around each particle acts as a sticking connector producing attractive forces.

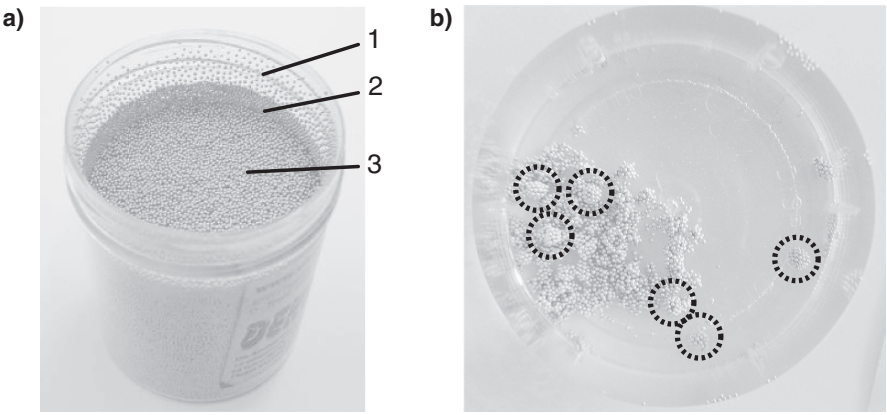

Fig. 8.15 Self-assembly of millimeter scale particles. (**a**) 0.5 mm beads in a cup. (**b**) In water, aggregating into spherical clusters

The implication is that we need to be careful when relating our work to small scales. Although at small scales it might be possible to observe complete bottom-up self-assembly, this might not be the case at large scales.

8.4 Speculations About Life

An important goal of the growing field of self-assembly is the development of a better formal understanding of the specific mechanisms and general principles underlying it. It is clear that the discovery of principles, which hold at all scales will require substantial input from various fields. At the molecular scale, biological systems are one of the examples that achieve robust self-assembly through an intricate web of well ordered reactions. Attention must be paid to the fact that all components are passively interacting even if it looks as if they are actively reacting. To achieve highly autonomous self-assembly modules, the realization of a sufficient number of degrees of freedom that are controllable is necessary for such small scale autonomous-distributed systems. In particular, because of the difficulty in including different types of attractive forces within the same system, realizing a new kind of connection mechanism endows the module with a better means of reacting in the environment. In this sense, the idea of a connector exploiting the thermoelectric effect may open yet another possibility for the state-of-the-art of self-assembly systems.

Figure 8.16 illustrates the level of autonomy realized as a system depending on the fragmentation of information (X-axis) and the total amount of information (Y-axis). We consider life as a kind of self-regulative system. Towards this goal, the system must be "self-observable." More specifically, the system must react differently according to the input depending on its internal state (memory). This is comparable to reactive systems but considered to have a slightly higher autonomy level. We speculate that there must be an adequate level of how to fragment information to the system (neither too heterogeneous nor too homogeneous, X-axis). And the system requires a certain amount of information to realize highly autonomous behavior (Y-axis).

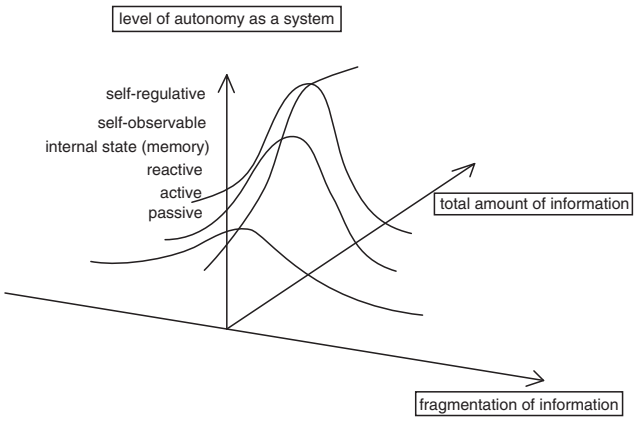

Fig. 8.16 The level of autonomy realized as a system depending on the fragmentation of information (X-axis) and the total amount of information (Y-axis)

Focusing on the mechanisms of living things from a viewpoint of autonomous and distributed systems, it can be noticed that the components which form the morphology are not always highly autonomous [40]. When we discuss autonomy of components in the context of autonomous-distributed systems, the crucial point might not be whether the units are passive or active, but whether the units are passive or "reactive" (Indeed, we could probably obtain the same results by employing modules without vibration motors, but by supplying power through an external, rotating magnetic field, Sect. 8.3.2.3). By drawing from our current experience in designing, constructing, and controlling macroscopic modular systems, we hope that we will be able to derive conclusions about the level of autonomy that is needed to achieve self-assembly. One could say that life is a blind engineer, because the components – e.g., molecules – self-construct into organisms in a completely bottom-up fashion.

Acknowledgments

The authors greatly thank Nathan Labhart, Flurin Casanova, and Marco Kessler for many helpful suggestions. This research is supported by the Swiss National Science Foundation project #200021-105634/1.

References

1. Leiman, P.G., Kanamaru, S., Mesyanzhinov, V.V., Arisaka, F., Rossmann, M.G.: Structure and morphogenesis of bacteriophage t4. Cellular and Molecular Life Sciences **60**, 2356–2370 (2003)
2. Zlotnick, A.: Theoretical aspects of virus capsid assembly. Molecular Recognition **18**, 479–490 (2005)
3. Fukuda, T., Kawauch, Y.: Cellular robotic system (cebot) as one of the realizations of self-organizing intelligent universal manipulator. In: Proc. Int. Conf. on Robotics and Automation, pp. 662–667 (1990)
4. Nakano, K., Uchihashi, S., Umemoto, N., Nakagama, H.: An approach to evolutional system. In: First IEEE Conference on Evolutionary Computation (1994)
5. Chirikjian, G.S.: Kinematics of a metamorphic robotic system. In: Proc. Int. Conf. on Robotics and Automation, pp. 449–455 (1994)
6. Murata, S., Kurokawa, H., Kokaji, S.: Self-assembling machine. In: Proc. Int. Conf. on Robotics and Automation, pp. 441–448 (1994)
7. Murata, S., Kurokawa, H., Yoshida, E., Tomita, K., Kokaji, S.: A 3-D self-reconfigurable structure. In: Proc. Int. Conf. on Robotics and Automation, pp. 432–439 (1998)
8. Murata, S., Tomita, K., Yoshida, E., Kurokawa, H., Kokaji, S.: Self-reconfigurable robot. In: Proc. Int. Conf. on Intelligent Autonomous Systems, pp. 911–917 (1999)
9. Yim, M.: New locomotion gaits. In: Proc. Int. Conf. on Robotics and Automation, vol. 3, pp. 2508–2514 (1994)
10. Kotay, K., Rus, D., Vona, M., McGray, C.: The self-reconfiguring robotic molecule. In: Proc. Int. Conf. on Intelligent Robots and Systems, vol. 1, pp. 424–431 (1998)
11. Rus, D., Vona, M.: Crystalline robots: Self-reconfiguration with compressible unit modules. Autonomous Robots **10**(1), 107–124 (2001)

12. Castano, A., Behar, A., Will, P.M.: The conro modules for reconfigurable robots. IEEE/ASME Transactions on Mechatronics **7**(4), 403–409 (2002)
13. Jorgensen, M.W., Ostergaard, E.H., Lund, H.H.: Modular atron: Modules for a self-reconfigurable robot. In: Proc. Int. Conf. on Intelligent Robots and Systems, vol. 2, pp. 2068–2073 (2004)
14. Zykov, V., Mutilinaios, E., Adams, B., Lipson, H.: Self-reproducing machines. Nature **435**(7039), 163–164 (2005)
15. Penrose, L.S.: Self-reproducing. Scientific American **200–206**, 105–114 (1959)
16. Hosokawa, K., Shimoyama, I., Miura, H.: Dynamics of self-assembling systems: Analogy with chemical kinetics. Artificial Life **1**(4), 413–427 (1994)
17. Hosokawa, K., Shimoyama, I., Miura, H.: 2-d micro-self-assembly using the surface tension of water. Sensors and Actuators A **57**, 117–125 (1996)
18. Bowden, N., Terfort, A., Carbeck, J., Whitesides, G.M.: Self-assembly of mesoscale objects into ordered two-dimensional arrays. Science **276**, 233–235 (1997)
19. Grzybowski, B.A., Mechal Radkowski, Campbell, C.J., Lee, J.N., Whitesides, G.M.: Self-assembling fluidic machines. Applied Physics Letters **84**, 1798–1800 (2004)
20. Grzybowski, B.A., Stone, H.A., Whitesides, G.M.: Dynamic self-assembly of magnetized, millimetre-sized objects rotating at a liquid-air interface. Nature **405**, 1033 (2000)
21. Grzybowski, B.A., Winkleman, A., Wiles, J.A., Brumer, Y., Whitesides, G.M.: Electrostatic self-assembly of macroscopic crystals using contact electrification. Nature **2**, 241–245 (2003)
22. Saitou, K.: Conformational switching in self-assembling mechanical systems. IEEE Transactions on Robotics and Automation **15**, 510–520 (1999)
23. White, P., Kopanski, K., Lipson, H.: Stochastic self-reconfigurable cellular robotics. In: Proc. Int. Conf. on Robotics and Automation, vol. 3, pp. 2888–2893 (2004)
24. White, P., Zykov, V., Bongard, J., Lipson, H.: Three dimensional stochastic reconfiguration of modular robots. In: Proc. Int. Conf. on Robotics Science and Systems, pp. 161–168 (2005)
25. Shimizu, M., Ishiguro, A.: A modular robot that exploits a spontaneous connectivity control mechanism. In: Proc. Int. Conf. on Robotics and Automation, pp. 2658–2663 (2005)
26. Bishop, J., Burden, S., Klavins, E., Kreisberg, R., Malone, W., Napp, N., Nguyen, T.: Programmable parts: A demonstration of the grammatical approach to self-organization. In: Proc. Int. Conf. on Intelligent Robots and Systems, pp. 3684–3691 (2005)
27. Griffith, S., Goldwater, D., Jacobson, J.: Robotics: Self-replication from random parts. Nature **437**, 636 (2005)
28. Mao, C., LaBean, T.H., Reif, J.H., Seeman, N.C.: Logical computation using algorithmic self-assembly. Nature **407**, 493–496 (2000)
29. Rothemund, P.W.K.: Folding DNA to create nanoscale shapes and patterns. Nature **440**(7082), 297–302 (2006)
30. Seeman, N.C.: DNA in a material world. Nature **421**, 427–430 (2003)
31. Shih, W.M., Quispe, J.D., Joyce, G.F.: A 1.7-kilobase single-stranded dna that folds into a nanoscale octahedron. Nature **427**, 618–621 (2004)
32. Winfree, E., Liu, F., Wenzler, L.A., Seeman, N.C.: Design and self-assembly of two-dimensional dna crystals. Nature **394**, 539–544 (1998)
33. Yokoyama, T., Yokoyama, S., Kamikado, T., Okuno, Y., Mashiko, S.: Selective assembly on a surface of supramolecular aggregates with controlled size and shape. Nature **413**, 619–621 (2001)
34. Boncheva, M., Ferrigno, R., Bruzewicz, D.A., Whitesides, G.M.: Plasticity in self-assembly: Templating generates functionally different circuits from a single precursor. Angewandte Chemie International Edition **42**, 3368–3371 (2003)
35. Gracias, D.H., Tien, J., Breen, T.L., Hsu, C., Whitesides, G.M.: Forming electrical networks in three dimensions by self-assembly. Science **289**, 1170–1172 (2000)
36. Wolfe, D.B., Snead, A., Mao, C., Bowden, N.B., Whitesides, G.M.: Mesoscale self-assembly: Capillary interactions when positive and negitive menisci have similar amplitudes. Langmuir **19**, 2206–2214 (2003)

37. Miyashita, S., Kessler, M., Lungarella, M.: How morphology affects self-assembly in a stochastic modular robot. In: IEEE International Conference on Robotics and Automation, pp. 3533–3538 (2008)
38. Pfeifer, R., Scheier, C.: Understanding intelligence. MIT, Cambridge (2001)
39. Hayakawa, J. (ed.): Time of an elephant, time of a mouse. CHUO-KORON-SHINSHA (1992)
40. Alberts, B., Hohnson, A., Lewis, J., Raff, M., Roberts, K., Walter, P.: Molecular biology of the cell. Garland Science, UK (2002)